NDT DETECTION OF DECAY AREAS AND EVALUATION OF THEIR ATTRIBUTES

P. Kapsalas[a*], M. Zervakis[b], P. Maravelaki-Kalaitzaki[c], E.T Delegou[d], A. Moropoulou[d]

[a]*National Technical University of Athens, Department of Electrical & Computer Engineering, Athens 15780, Greece*
[b]*Technical University of Crete, Department of Electronics & Computer Engineering, Chania 73100, Greece*
[c]*Ministry of Culture, 25th Ephorate of Prehistoric & Classical Antiquities, Chania 73100, Greece*
[d]*National Technical University of Athens, School of Chemical Engineering, Athens 15780, Greece*

Abstract

The systematic analysis of corrosion damage on cultural heritage objects is an aspect of multidisciplinary interest. The application of computer-aided approaches in corrosion control has recently become a challenging issue. However, the majority of researches attain to estimate the decay presence by evaluating colour and texture alterations. This paper is geared towards investigating non-destructive detection and quantification of stone degradation by using machine vision schemes. The contribution of the current work is 4-fold. Thus, (1) several detection schemes were developed, each handling in a different way the background in-homogeneity. (2) Numerous statistical metrics were introduced to quantify corrosion damage. These metrics mainly consider the decay areas size, spatial distribution, shape and darkness. (3) The potential of several monitoring modalities in determining corrosion attributes is studied, and (4) the corroded areas' shape features are considered in association with the cleaning and structural state that they represent.

1. Introduction

The most frequently observed corrosion phenomena encountered on sheltered surfaces is black crust. Black crust is mainly associated with the formation of gypsum ($CaSO_4.2H_2O$). Further to the discoloration of stonework, black crusts also accelerate degradation phenomena due to their catalyzing activity. The colour alterations, as well as the structural effects on the stone material, are dependent upon the duration of exposure and the chemical composition of the substrate. The most frequently encountered constituents in black crusts are carbonaceous particles, heavy metals, calcite, silicates, potassium nitrate and various organic compounds in lower concentrations [1].

Black crusts do not form homogeneous varnished layers, but are rather composed of small black particles sporadically located within the matrix of encrustation [1]. These black particles are responsible for the coloration of the crust. Small white particles, often observed in the body of black crusts, are mainly associated with the presence of gypsum crystals and re-crystallized $CaCO_3$. All these aspects indicate that chemical cleaning is important not only for the restoration of aesthetical damage but also for preventing further degradation, which may lead to structural disintegration and loss of stone material. In order to select the appropriate cleaning approach and the time of intervention, an accurate diagnosis process should be followed. The diagnostic procedures employed thus far involve ablation of the specimen under consideration and subsequent chemical analyses to assess the severity of degradation and the type (composition) of deposits. However, this process is destructive to the material, so that the development of non-destructive approaches able to provide reliable results on both the severity and the type of degradation is an issue of great importance.

1.1 Related Work

Non-destructive analysis methodologies provide powerful tools in the fields of material science and artwork analysis. These techniques have been extensively used recently for characterizing the cleaning state and/or the structural integrity of aerospace materials. However, little work has been done in assessing corrosion damage on stonework. The intricacy of the problem stems from the specific features of corrosion phenomena i.e. influences of various pollutant factors along with the great diversity of litho-type and the corresponding variations on decay phenomenology. An early attempt to segment degraded areas on metals was performed in [2], where decay effects are inspected by eddy currents and infrared thermography. The information gathered is subsequently fused with the use of statistical and/or probabilistic algorithms. More recent researches [3] approach corrosion damage on metals by introducing morphological analysis of decay patterns to aid the characterization and classification of deterioration type. A related study reported in [4] is focused towards recognizing the various defects encountered on a cold mill strip. Several Image Processing (IP) techniques have been developed for identifying and reconstructing corrosion damage on old paintings [5]. IP approaches have been also partially employed to detect decay effects on stonework. In [6], back-scattered electron images obtained with scanning electron microscopy-energy dispersive X-rays analysis were used to identify and quantify salts and porosity with depth in porous media. Moreover, methods for characterizing the stone structure and detecting regions of material loss were developed in the study of Moltedo et al. [7], while Boukouvalas et al. [8] introduced computer vision techniques for the detection and classification of mineral veins on ceramic tiles surfaces.

Besides the comparison of several algorithmic approaches, we also investigate how exposure or even cleaning conditions are reflected in the size and the relative intensities of corroded areas (over the background). This aspect is approached by using statistical tests to assess the significance of differences observed in the decay characteristics of the examined structures. These tests also contribute in evaluating the efficiency of chemical cleaning as well as in understanding the procedures of decay evolution. The testing framework involves image data sets of degraded stone surfaces screened by the Fiber Optics Microscope (FOM), Reflectography in the visible spectral band and Digital Camera. Shape features of the segmented decay areas are also a significant characteristic, which has been studied throughout this work. The initial objective of our approach is to investigate whether the structural or cleaning state are reflected onto the decay areas shape.

2. Problem Specification

2.1. Experimental Setup

The studied images represent degraded stone regions monitored via a FOM, a reflectography system operating at the visible spectral band and a digital camera. The FOM images depict sheltered and unsheltered areas obtained from the columns of the National Archaeological Museum (Athens),

---

Corresponding author: Kapsalas Petros
mailto:pkaps@image.ece.ntua.gr

while the digital camera images represent a stone specimen depicting adjacent cleaned and uncleaned stripes. The FOM images are further subdivided (due to their location) into reedings and flutings, to study the different degradation and structural effects encountered on surfaces of different exposure to weathering conditions. Thus, reedings represent areas more exposed to the rain and winds' action and consequently the black crusts occurring on these areas tend to be thinner than the corresponding crusts encountered on the adjacent flutings surfaces. On the other hand, unsheltered surfaces tend to develop more lamellar texture and crusts thinner in thickness. The latter observation can be explained by taking into account the water activity that results in removing the deposited materials. In this work, the cleaning effects are evaluated in terms of 4 well-known cleaning interventions. Namely we have employed (a) an ion-exchange resin paste with de-ionized water (DS); (b) a biological paste (BP), (c) a WMB approach and an Nd:Yag laser cleaning system. The potential and the limitations of these methods have been investigated in greater detail in our previous works [11], [9], [10]. The severity of degradation is assessed in terms of the size of the detected decay areas and the alteration of the relative (over the background) intensities on areas of corrosion damage.

Aiming at studying the effectiveness of the segmentation algorithms in detecting various types of corrosion defects we selected representative images, where we also extracted the Ground Truths (GTs). The images were selected with the aid of the experts, to reflect the deterioration encountered in a variety of environmental conditions [9].

3. Overview of the Developed System

As it was stated in the introduction of the paper, the detection problem is approached by developing several image segmentation schemes to determine accurately the exact location, size and shape of decay areas [9]. The implementation of an automated framework to derive the GTs and evaluate the efficiency of the detection approaches is also supported in our system. Finally a shape analysis methodology was implemented to investigate the associations between decay areas shape and the structural or cleaning state that they represent. Section 3 discusses briefly the operations supported in this work.

3.1. Overview of the Detectors Architecture

In an effort to design an effective detection scheme several aspects associated with the potential of the monitoring system and the structural features of the stone material should be considered. Thus, the detection scheme should be well adapted to the expected extent and shape features of the decay patterns. A further issue is the background structure on locations where decay patterns occur. The typically low contrast between decay areas and the background, which sometimes approximates the in-homogeneity contrast of the stone structure, itself, should also be carefully considered. Furthermore, due to the growth of the decay areas, there is no lower bound to this contrast. Obviously, the segmentation algorithm must be as sensitive as possible to the systematic variations caused by decay areas presence while suppressing all these random variations induced by noise and by the background stone structure. This means that the detection approach should take into account dynamically the intensity distribution of the local background. To provide robust segmentation results, the peculiarities of the problem must be thoroughly considered in the design of effective segmentation approaches.

Based on the above specifications, we have developed several algorithmic schemes each of which considers in a different way the background in-homogeneity. Thus, the implemented algorithms can be classified into different categories depending on the way that they handle the background in-homogeneities [9]. The first step towards the implementation of an efficient spot detector is to decouple the detection of useful information from the background activity. This is achieved by the first algorithmic approach, which employs a broadband high-pass filter to enhance the decay areas location and remove the general structure of the background. The segmentation process in this first approach is conducted through a simple thresholding technique that sets a global threshold from the statistical analysis of the entire image. The disability of such methods to eliminate the induction of false positive and false negative spots leads to the employment of the next category that uses adaptive thresholding schemes. Thus, we tested algorithmic approaches that perform thresholding based on characteristics of the local background structure using also some knowledge of the extent and spatial arrangement of decay patterns. All the above methods, however, use information from the histogram of the sub-regions in order to select an appropriate threshold. A fundamental limitation of such approaches is that they completely ignore information regarding the spatial relations of intensity values. In order to overcome this limitation, we also tested a local region growing segmentation approach. The basic goal here is to select local thresholds dynamically, based on an iterative evaluation of the labeling quality achieved by each threshold value. At each iteration, the initially selected area is grown according to a thresholding similarity predicate aiming at producing compact areas, while avoiding the merging of different regions. In an effort to further reduce the segmentation errors introduced due to the local background variations, we also implemented a more elaborate growing scheme that uses prior knowledge of the expected size of spots and the inter-spot distance. This procedure is quite reliable in detecting spot locations even in low contrast between the spot and its background. However, the detected shape is distorted and the boundary of the individual spots is smoothed. In order to address the effective shape detection of decay spots, we tested a category of local morphological operators. This approach preserves the original spot shape, at the price of more false positive spots and merged spots that should be separated. In order to exploit the strength of both concepts (accurate topology detection and shape preservation) a morphological fusion algorithm was implemented that expands the areas detected by the local region growing approach up to the size derived by the morphological operators [9], [10], [11].

3.2. Evaluate the Potential of the Detection Schemes

Our work estimates the robust points and the drawbacks of each detection methodology through an automated framework, which was built to perform this task objectively. This framework guarantees reliable and objective estimation of segmentation algorithms' performance while it allows informed experimental feedback for the design of improved segmentation schemes. As it could be expected, the responses of the tested detection schemes divert in their potential to approach the topology, extent and shape of decay areas [9]. More specifically, some of them tend to split segments into adjacent small in size spots. Others succeed in providing reliable information concerning the topology of decay patterns, while distorting their extent and shape. The objective of the performance evaluation stage is to assess the potential and the limitations of the recruited algorithmic schemes in segmenting degradation patterns, while exploiting individual features associated with the robust points and the drawbacks of each approach.

3.2.1. Ground Truth Matrix Extraction

The extraction of (GT) involves fusion of the areas segmented by all the algorithms. The fusion takes place by examining the implemented algorithms in pairs and extracting the overlapping segments. The non-overlapping segments obtained at each stage are subsequently checked towards the results of a consecutive algorithm. The process proceeds until all methods have been examined. Figure 2 shows that the Ground Truth stems from the union of the Non-Overlapping (obtained when the process terminates) and the total overlapping labels, derived at each step of the extraction approach. Through a brief visual inspection of the segmented degraded regions, it can be verified that the total overlapping patterns, correspond to areas larger in extent than the non-overlapping. However, the experts considered that the non-overlapping areas should also be present in the Ground Truth as these spots correspond to regions that are likely to represent decay effects. Figure 2 illustrates the steps followed to determine the Ground Truth Matrix. The process identified under the term "Manage Segmented Areas" corresponds to the procedure illustrated in figure 1.
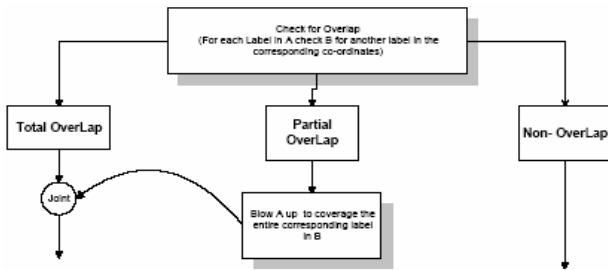

Figure 1: Check for overlap spots and processing the partially overlapping labels.
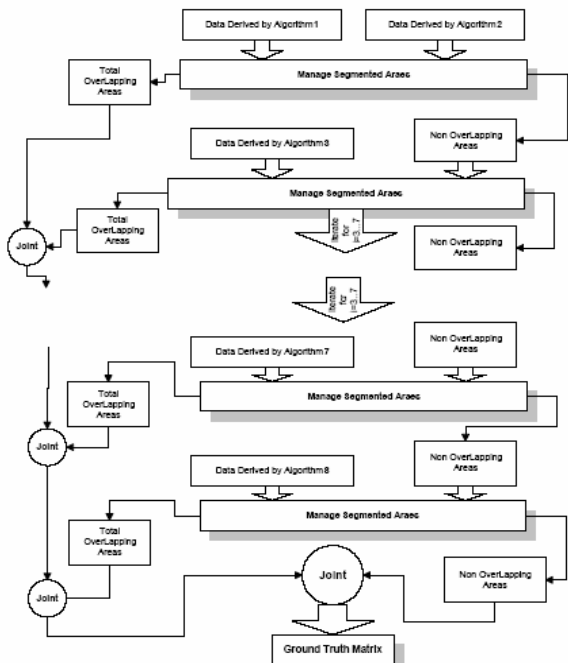

Figure 2: Flowchart of the Ground Truth Extraction Approach.

3.3.2.   Performance Evaluation

The segmentation of an image through an algorithmic approach (AS) is compared towards the Ground Truth (GT) specification of that image to count instances of correct segmentation, under-segmentation, over-segmentation, missed regions, and noise regions. The algorithms' performances and

their potential are estimated, in this work, through studying the Receiver Operating Characteristic (ROC) curves [9]. The ROC curves are obtained by modifying the thresholds within meaningful ranges and subsequently calculating instances of correct and incorrect segmentation.

3.3.   Extraction of Shape Features

Following to the detection of the areas of interest and the determination of their boundaries, we also extract boundary sequences as contour-based shape representations. The boundary sequences are defined as an ordered sequence of boundary pixel locations in clockwise order. The extraction method has proven to work well even if a shape has holes.

3.3.1. Shape Features from Boundary Sequences

In this section we provide an overview of the boundary sequence extraction approach employed to detect hole regions and nested areas within segments. According to the literature, if a region R includes holes $H_1, H_2, \cdots H_m$ then it can be expressed as:

$$BD(R): BS(R) \rightarrow BS(H_1) \rightarrow \cdots \rightarrow BS(H_m)$$

The boundary sequence extraction method scans the image in a raster-scan manner as in TV. There are three different states of current scan pixel, p in a scan line as follows and the state transition diagram is presented in the figure below.

$$S_0 : p \in \quad background \quad region$$
$$S_1 : p \in \quad foreground \quad region$$
$$S_2 : p \in \quad hole \quad region$$

The state transition diagram is initialized when a new line starts and finishes at location of end-pixel in the scan line starts (state E).
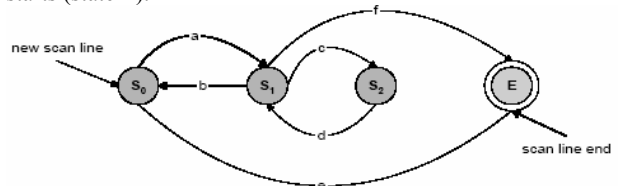

Figure 3: State Transition Diagram

When a new object region or a new hole region is extracted, pixels of extracted boundary sequence are marked with appropriate label that is assigned differently to each object region and each hole region. The boundary sequence can be extracted by a boundary following operation [12]. A nested hole counter is used to determine which state is the next one when a background pixel is found in S_1. The transition conditions are summarized as follows.

- **a, d:** When a foreground or a labeled pixel is met.
- **b:** When a background pixel is met and the nested   count is zero.
- **c:** When a background pixel is met and the nested count is not zero.
- **e:** When there remain only the background pixels in the current scan line.
- **f:** When no background pixel is found. In each state, following operations are performed.
- **S_0:** When a foreground pixel is found, a new boundary descriptor for the new object region is generated through boundary following.
- **S_1:** When a background pixel is found, a new hole boundary sequence for the hole region is generated through boundary following. The hole boundary sequence is attached to appropriate boundary descriptor.
- **S_2:** When a foreground pixel is found, a new boundary descriptor for the new object region in a hole is generated

When the segments' boundary sequence is extracted the perimeter, compactness and moments can be easily computed. The Euler number is defined as the number of components minus the number of holes in region R.

$$E = 1 - N(H) \qquad (1)$$

The presented results summarize our system's response when dealing with surfaces of different degradation state. Subsequently, we investigate the algorithms' potential to detect decay on images acquired through various monitoring modalities capturing decay characteristics at various scales. A further issue approached through statistical evaluation is the cleaning state and/or the conditions of exposure and whether they are reflected on the size of corroded areas and their relative intensities over the background. Due to their stochastic distributions, the alterations on the darkness of decay spots are investigated through t-tests, while alterations on decay patterns' sizes are examined through non-parametric rank sum tests (Mann Whitney U-test). Finally, at the end of the results section we briefly discuss the associations between the degradation state and the corresponding decay areas shape.

4. Results

Through this work, the evaluation of the algorithmic results is performed by both qualitative and quantitative means. Visual evaluation implies inspection of the segmentation results by the experts. The examined properties are the existence of true decay spots as well as their size and shape. The visual evaluation has been performed on the basis of 45 FOM images. Statistical evaluation is performed using several statistical metrics to assess the severity and extent of degradation.

4.1. Visual Inspection and Quantification of Decay

This section presents and discusses several results, demonstrating the performance of the employed detection schemes. Figures 4 and 5 depict black crust located on a sheltered and unsheltered fluting respectively. It is readily observed that the algorithms sufficiently distinguish the deterioration patterns related to the presence of black and white particles. According to the experts, the detected areas (number and size) are in good accordance with their own judgment of deterioration patterns prevalence in the image [11]. Even the spatial distribution of small black particles, which are derived by the algorithm in the vicinity of polished sections of black crusts, are expected in such formations. A further study of the detection results illustrated on figures 4 and 5 reveals that larger number of decay patterns is segmented on sheltered untreated flutings.
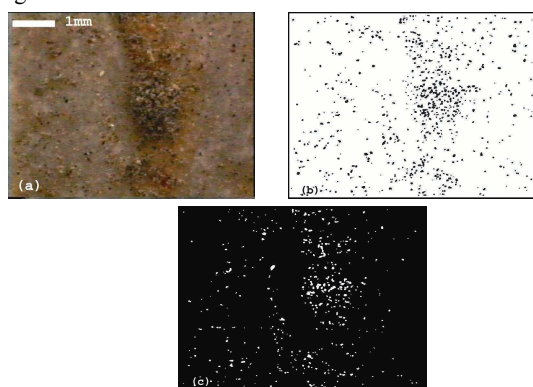

Figure 4: (a) Sheltered untreated Fluting monitored by FOM, (b) black particles detected on (a), (c) white particles detected on (a).

Such assessments are in accordance with the experts' judgments [11]. The detection results derived when studying treated surfaces are also visually inspected by the experts and is evidenced that that the deterioration patterns are eliminated after

the application of chemical cleaning methods [10]. At this point we should state that the images presenting deterioration state after chemical cleaning illustrate areas adjacent to the untreated black crust shown in figures 5 and 6.
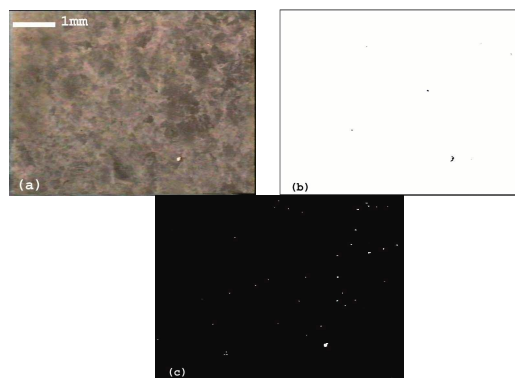

Figure 5: (a) Unsheltered untreated Fluting monitored by FOM, (b) black particles detected on (a), (c) white particles detected on (a).

The degradation phenomena on the studied images are quantified by measuring the number of spots, the percentage of area covered by such spots and their average size and spatial distribution. In order to increase the reliability of statistical measures concerning the spatial distribution of spots prior and after cleaning with various methods, we adopt a statistics consideration on many image sub-regions. Table 1 depicts the percentage of surface covered by black particles. Several conclusions can be drawn from the results of Table 1. Sheltered surfaces and flutings show more severe degradation phenomena than their unsheltered counterparts. These results can reasonably well be interpreted by the fact that sheltered areas and column flutings accumulate the atmospheric deposition, while unsheltered areas and column reedings, being more exposed to rain and wind action, show lower amounts of decay effects. The qualitative (visual) and quantitative measures extracted from our analysis methodology can be further used to assess the capability of chemical intervention methods [11].

Table 1: Mean percentage of the studied surface covered by black particles

	Diagn.	BP	DS (30 min)	DS (60min)	WMB
Shelt. Flut	3.75	0.04		0.45	0.04
Shelt. Reed.	1.73	0.05		0.06	
Unshel. Flut	0.53		0.04		
Unshel. Reed.	0.29		0.04		0.02

4.1.1. Inspection by Various Monitoring Modalities

As it was stated previously, one of the objectives of this work was to assess the effectiveness of the implemented algorithms under different monitoring systems [11]. Figure 6(a) illustrates a stone surface depicted by the digital camera, while (b) and (c) shows the segmented black and white spots. Figures 7 (a) through (c) depict the same surface monitored under the reflectography in the visible spectral band and the black and white particles detected on it. As it can be seen, treated and untreated stripes co-exist on the stone specimen.
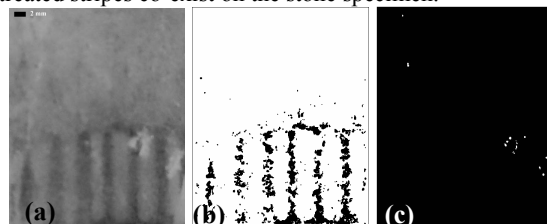

Figure 6: (a) Stone material (monitored by a digital camera) demonstrating cleaned and un-cleaned stripes, (b) Black particles detected, (c) white particles detected.

Optical inspection by the experts on Figures 6 and 7 verifies that the topology of the detected black particles, their spatial distribution as well as their shape and size closely resemble to their own judgment of sporadic particle presence. A more dissect inspection of Figures 6(c) and 7(c) though, reveals the detection of white decay spots even on treated regions. According to the experts' assessment, these spots are associated to regions of material loss. The above false positive induction illustrates the inability of the monitoring systems to distinguish between areas where gypsum prevails and other areas where material loss occurs. This limitation arises from its low magnification rate as it becomes difficult to view the inter particle area between adjacent black spots and thus to accurately locate areas of gypsum or $CaCO_3$ presence. A further explanation of the false positive detection is associated to the operation of the reflectography screening system and is discussed in more detail in [11].
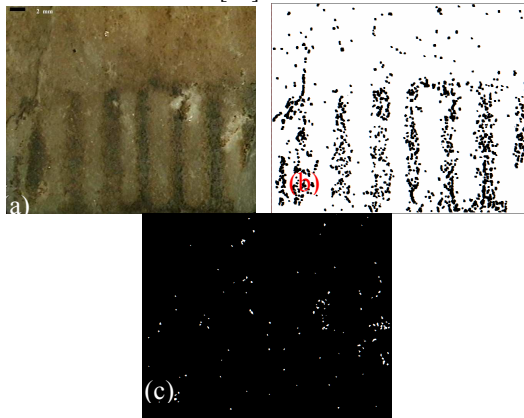

Figure 7: (a) Stone material (monitored by a refectography system (vis)) demonstrating cleaned and un-cleaned stripes, (b) Black particles detected, (c) white particles detected.

4.2. Tests of Statistical Significance

Visual evaluation of the segmentation results verified that the main attributes of corrosion that are significantly altered due to cleaning or exposure conditions are the sizes of the decay areas and their relative darkness over the background. More specifically, it was revealed that more severe degradation phenomena are basically associated with the presence of larger in extent and darker corrosion patterns. To establish the occurrence of such associations, we employ tests of statistical significance to prove or disprove the existence of alterations. The significance of alterations on the sizes of decay patterns is assessed through the Mann Whitney U-test, while intensity variations are considered through t-tests.

In both the parametric and the non-parametric tests we always consider as null hypothesis that the first of the two populations has a distribution of intensities or area sizes laid on lower levels, while the alternative hypotheses claims the opposite. To prove or disprove the tested hypotheses we use one-sided statistical test. Thus, when the t-value or the U-value is larger than the critical values, then the null hypothesis is rejected in favor of the alternative hypothesis, supporting the claim of different distributions. Tables 2 and 3 summarize the results derived after the application of the T-test and the Mann-Whitney U-test respectively. The results presented in tables 2 and 3, reveal that the cleaning methods attain to eliminate significantly the size of corrosion patterns and their relative darkness over the background. This observation is valid for almost all tests (cleaning strategies), except for the case where unsheltered reedings are cleaned by the DS method. This supports the conclusions derived by the chemical analysis [11], according to which DS performs only mild cleaning and minimizes material loss. Furthermore, according to the results,

the black particles detected on sheltered flutings are always larger in size and darker than the corresponding spots detected on any other of the studied surfaces. Moreover, table 2 reveals that decay patterns segmented on sheltered flutings are darker than the corresponding patterns detected on sheltered reedings. An effort to investigate whether a similar observation is also valid for the unsheltered areas revealed that the observed differences on the relative intensity values among unsheltered flutings and reedings is marginally significant (test 10, table 2). This conclusion also agrees to the chemical reports [11].

Table 2: Comparative study on the significance of intensity alterations.

		Algorithmic Response
1.	Shelt. Flut. (Ds) (vs) Shelt. Flut. (Diag.)	Df= 34 Crit t (1-tail)=1.691 **t= 25.76**
2.	Shelt. Flut. (WMB) (vs) Shelt. Flut. (Diag.)	Df= 33 Crit t (1-tail)=1.692 **t= 62.41**
3.	Shelt. Flut. (BP) (vs) Shelt. Flut. (Diag.)	Df= 27 Crit t (1-tail)=1.703 **t= 33.90**
4.	Shelt. Reed. (Ds) (vs) Shelt. Reed. (Diag.)	Df= 9 Crit t (1-tail)=1.833 **t= 12.59**
5.	Shelt. Reed. (BP) (vs) Shelt. Reed. (Diag.)	Df= 8 Crit t (1-tail)=1.860 **t= 12.72**
6.	Shelt. Reed. (Diag.) (vs) Shelt. Flut. (Diag.)	Df= 28 Crit t (1-tail)=1.701 **t= 13.44**
7.	Unshel. Flut. (Diag.) (vs) Shelt. Flut. (Diag.)	Df= 34 Crit t (1-tail)=1.691 **t= 47.96**
8.	Unshel. Flut. (DS) (vs) Unshel. Flut. (Diag)	Df= 22 Crit t (1-tail)=1.717 **t= 7.75**
9.	Unshel. Flut. (Diag.) (vs) Shelt. Reed. (Diag.)	Df= 16 Crit t (1-tail)=1.746 **t= 16.35**
10.	Unshel. Reed. (Diag) (vs) Unshelt. Flut. (Diag.)	Df= 22 Crit t (1-tail)=1.717 **t= 4.57**
11.	Unshel. Reed. (Ds) (vs) Unshelt. Reed. (Diag.)	Df= 9 Crit t (1-tail)=1.833 **t= 7.57**
12.	Unshel. Reed.(WMB)(vs) Unshelt. Reed. (Diag.)	Df= 9 Crit t (1-tail)=1.833 **t= 8.42**

Table 3: Comparative study on the significance of decay areas size alterations

		Algorithmic Response
1.	Shelt. Flut. (Diag) (vs) Shelt. Flut. (Ds)	N_1=24 N_2=12 (U=252 U_{crit}=74) **P= 5.92*10^{-5}**
2.	Shelt. Flut. (Diag) (vs) Shelt. Flut. (WMB)	N_1=24 N_2=6 (U=144 U_{crit}=27) **P=1.6x10^{-6}**
3.	Shelt. Flut. (Diag) (vs) Shelt. Flut. (BP)	N_1=24 N_2=6 (U=144 U_{crit}=27) **P= 1.6x10^{-6}**
4.	Shelt. Reed. (Diag) (vs) Shelt. Reed. (DS)	N_1=6 N_2=6 (U= 36 U_{crit}=3) **P=10.8x10^{-4}**
5.	Shelt. Reed. (Diag) (vs) Shelt. Reed. (BP)	N_1=6 N_2=6 (U= 36 U_{crit}=3) **P=10.8x10^{-4}**
6.	Shelt. Flut. (Diag) (vs) Shelt. Reed. (Diag)	N_1=24 N_2=6 (U= 0 U_{crit}=27) **P=1.6x10^{-6}**
7.	Shelt. Flut. (Diag) (vs) Unshelt. Flut. (Diag)	N_1=24 N_2=12 (U=218 U_{crit}=74) **P=7.9x10^{-10}**
8.	Unshel. Flut. (Diag) (vs) Unshelt. Flut. (Ds)	N_1=12 N_2=12 (U=144 U_{crit}=31) **P=3.6x10^{-7}**
9.	Shelt. Reed. (Diag) (vs) Unshelt. Flut. (Diag.)	N_1=6 N_2=12 (U= 62 U_{crit}=9) **P= 6.7x10^{-3}**
10.	Unshel. Flut.(Diag) (vs) Unshel. Reed. (Diag)	N_1=12 N_2=6 (U= 72 U_{crit}=9) **P= 5.3x10^{-5}**
11.	Unshel.Reed. (Diag) (vs) Unshel. Reed. (Ds)	N_1=6 N_2=6 (U= 24 U_{crit}=3) **P= 0.19**
12.	Unsh. Reed.(Diag) (vs) Unshel. Reed.(WMB)	N_1=6 N_2=6 (U= 36 U_{crit}=3) **P= 10.8x10^{-4}**
13.	Shelt. Reed. (Diag) (vs) UnShelt. Reed.(Diag)	N_1=6 N_2=6 (U= 36 U_{crit}=3) **P= 10.8x10^{-4}**

4.3. Evaluating the Algorithms' Performance

In this work, we consider the ROC curves as robust measures for evaluating the algorithms' performance [9]. Throughout this subsection, we briefly discuss the performance curves derived for the most representative case of corrosion damage occurrence (sheltered untreated fluting). This case corresponds to a surface demonstrating a rapidly varying background structure. Figure 8 depicts the algorithms'

performance through the ROC curves and reveals that the Conditional Thickening and the Region Growing algorithms perform generally better than the others. This characteristic reflects the algorithms' potential to perform efficient detection irrespective of noise levels and variations over the background.
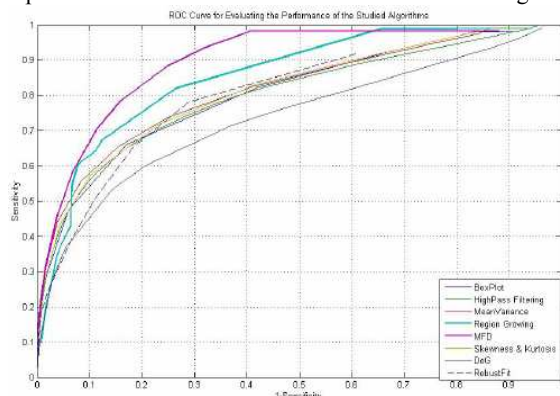

Figure 8: ROC curves depicting the performance of the implemented algorithms in the case of the sheltered untreated fluting (illustrated in figure 4).

4.4. Shape Features Analysis

As it was discussed earlier, an objective of the current work is to examine how the cleaning and structural conditions are reflected onto the shape of the segmented decay areas. An important feature revealed through our analysis, is the occurrence of hole-regions within segments. According to the experts this is a remarkable characteristic, which reflects the prevalence of discontinuities in the body of black crusts. More specifically humidity affects the structure of black crusts due to the dissolution of the gypsum. This phenomenon can be observed (in the micro-scopical scale) by the occurrence of white spots within the body of black crusts. Through this subsection we attempt to investigate associations between the occurrence of hole-regions and the exposure of the stone material/or its cleaning state. Thus, table 4 presents the fraction of decay areas including hole-regions. This measure provides an initial general view of the phenomenon.

Table 4: Percentage of the segmented decay patterns containing holes into their areas.

	Shelt. Untr. Flut.	Shelt. Untr. Reed.	Shelt. Clean. Areas (Flut.& Reed.)	Unshelt Untr. Flut.	Unshelt. Areas (Cleaned)
Percentage of labels containing holes (%)	4.97	2.29	0	0.88	0

Direction of the segmented decay areas, as an attribute of the corrosion state, is also evaluated. Thus, the decay areas orientation is considered through measuring the direction of their axis of least inertia [12]. Through this study, we attempt to estimate whether the decay patterns tend to be oriented towards specific directions. To investigate the occurrence of directionality we measure the standard deviation on the distributions of orientations. The derived results indicate that decay patterns prevailing on unsheltered areas tend to be more oriented than the corresponding patterns segmented on sheltered areas. This may reflect the effect of water's fluency.

5. Conclusions

This work is geared towards investigating aspects of non-destructive detection and quantification of corrosion damage on stonework. The studied surfaces are monitored via the aid of several imaging modalities. More specifically, we use a Fiber Optics Microscope (FOM), a Digital Camera, and a reflectography system operating at the visible spectral band.

Several algorithms are tested to detect decay patterns. Thus, one of the initial objectives of this work is to study the efficiency of the implemented algorithms in accurately determining the exact location of decay patterns, as well as their size and shape features. The performance of the algorithmic schemes is assessed through studying the ROC curves. From the performance evaluation [9] it is revealed that the efficiency of each algorithm is closely related to the background structure.

Further to validating the algorithms' performance, this work also investigates the efficiency of the cleaning interventions. Several statistical tests are employed to estimate whether the cleaning approaches attain to reduce the crusts' thickness and the extent of corroded areas. The results derived from the statistical tests indicate that all the cleaning methods attain to reduce the crusts thickness and the extent of the corroded areas. Furthermore, it is revealed that thicker crusts are encountered on sheltered untreated flutings. This conclusion is also in accordance to the experts' opinion.

Finally, we study whether the structural or cleaning effects are reflected onto the decay patterns shape. Our analysis revealed that corroded areas segmented on unsheltered areas tend to be oriented towards specific directions. Moreover, the occurrence of hole-regions in the segmented degradation patterns is also investigated. This work indicated that decay areas with more hole-regions prevail on areas of more severe degradation. According to the experts, this effect is closely related to the discontinuities encountered in black crusts and arises due to the dissolution of gypsum by the walls' humidity.

5. References

[1] Maravelaki-Kalaitzaki, P., Anglos, D., Kilikoglou, V., Zafiropoulos, V., 2001b: Compositional characterization of encrustation on marble with laser induced breakdown spectroscopy. *Spectrochim. Acta*, 56(6), pp. 887–903.

[2] Gros, X. E., Bousique, J., Takahashi K., 1999. NDT Data Fusion at Pixel Level. *NDT&E International*, 32(5), pp.283–292.

[3] Choi, K. Y., KIM, S. S, 2005. Morphological analysis and classification of types of surface corrosion damage by digital image processing. *Corros. Sci,,* 47(1), pp. 1–15.

[4] Kim, K. M., Park, J. J., Song, M. H., Kim, I. C., Suen, C. Y., 2004. Design of a binary decision tree for recognition of the defect patterns of cold mill strip using generic algorithm. In: *17th International Conference on Industrial and Engineer. Applications of Artificial Intelligence and Expert Systems*, pp. 341–350.

[5] Pappas, M., Pitas, I., 1998. Old painting digital color restoration. In: *Proc. of 1998 NOBLESSE Workshop on Non-Linear Model Based Image Analysis (NMBIA'98)*, pp. 188–192.

[6] Cardell, C., Yebra, A., Van-Grieken, R. E., 2002. Applying digital image processing to SEM-EDX and BSE images to determine and quantify porosity and salts with depth in porous media. *Microchim. Acta*, 140(1-2), pp. 9–14.

[7] Moltedo, L., Mortelliti, G., Salvetti, O., Vitulano, D., 2000. Computer aided analysis of buildings, *J. Cult. Herit. 1*(1), pp. 59–67.

[8] Boukouvalas, C., De-Natale, F., Natale, D., De-Toni G., Kittler, J., Marik, R., Mirmehdi, M., Petrou, M., Le-Roy, P., Salgari, R., Vernazza, G., 1998. Automatic system for surface inspection and sorting of tiles. *J. Mater. Process Tech. 82*(1-3), pp. 179–188.

[9] Kapsalas, P., Zervakis, M., Maravelaki-Kalaitzaki, P., 2007. Evaluation of Image Segmentation Approaches for Non-Destructive Detection and Quantification of Corrosion Damage on Stonework, *Intern. Journ. of Corr. Sci.,,* Accepted for publication.

[10] Kapsalas P., Maravelaki-Kalaitzaki P., Zervakis M., Delegou E.T, Moropoulou A. 2007. Optical Inspection for Quantification of Decay on Stone Surfaces, *NDT&E International,* 40 (1), 2007, pp.2-11.

[11] Kapsalas, P., Maravelaki-Kalaitzaki, P., Zervakis, M., Delegou, E.T., Moropoulou, A., 2006. A Morphological Fusion Algorithm for Optical Inspection and Quantification of decay Patterns on Stone Surfaces, *International Journal of Construction & Building Materials,* doi: 10.1016/j.conbuildmat.2006.08.024

[12] Ramesh, J., Rangachar, K., Brian, G., Schunck: "Machine Vision" *McGraw-Hill International Editions, Computer Science Series.*